analytical chemistry

pubs.acs.org/ac Article

Ratiometric Luminescence Aptasensor Based on Dual-Emissive Persistent Luminescent Nanoparticles for Autofluorescence- and Exogenous Interference-Free Determination of Trace Aflatoxin B1 in Food Samples

Lu-Ming Pan, Xu Zhao,* Xiang Wei, Li-Jian Chen, Chan Wang, and Xiu-Ping Yan*

Cite This: *Anal. Chem.* 2022, 94, 6387−6393 Read Online

ACCESS | Metrics & More | Article Recommendations | Supporting Information

ABSTRACT: Sensitive and accurate determination of aflatoxin B1 (AFB1) is of great significance to food safety and human health as it is recognized as the most toxic mycotoxin and carcinogenic. Herein, we report a ratiometric luminescence aptasensor based on dual-emissive persistent luminescent nanoparticles (PLNP) for the accurate determination of trace AFB1 in complex food samples without autofluorescence and exogenous interference. Dual-emissive PLNP $ZnGa_2O_4:Cr_{0.0001}$ was prepared first and acted as the donor for energy transfer as well as the signal unit with phosphorescence at 714 and 508 nm (the detection and the reference signal, respectively). AFB1 aptamer was then bonded on the surface of PLNP to offer specific recognition ability. Aptamer complementary DNA modified with Cy5.5 was employed as the acceptor for energy transfer and the quenching group to eventually develop a turn-on ratiometric luminescence aptasensor. The developed ratiometric luminescence aptasensor combined the merits of long-lasting luminescence, in situ excitation and autofluorescence-free of PLNP, exogenous interference-free and self-calibration reading of ratiometric sensor, as well as the high selectivity of aptamer, holding great promise for accurate determination of trace AFB1 in complex matrix. The developed ratiometric aptasensor exhibited excellent linearity (0.05−70 ng mL^{-1}), low limit of detection (0.016 ng mL^{-1}), and good precision (2.3% relative standard deviation for 11 replicate determination of 1 ng mL^{-1} AFB1). The proposed ratiometric aptasensor was successfully applied for the determination of AFB1 in corn, wheat, peanut, millet, oats, and wheat kernels with recoveries of 95.1−106.5%.

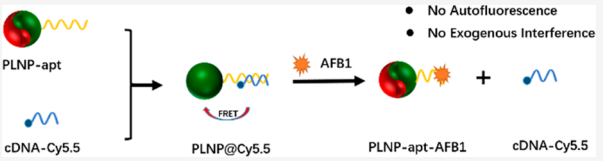

INTRODUCTION

Aflatoxin B1 (AFB1), a secondary metabolite of *Aspergillus flavus* and *A. parasiticus*, is the most toxic mycotoxin known as far with strong carcinogenic and teratogenic effects and listed as a Class 1A carcinogen by the International Agency for Research on Cancer.[1−3] It has good thermal and chemical stability and is widely found in corn, peanut, soybean, wheat, and other grains.[4,5] Many countries and regions have strict requirements on the content of AFB1 in food, for example, the European Union has established a maximum allowable content of AFB1 in cereals to 2 $\mu g\ kg^{-1}$.[6−8] Therefore, it is imperative to establish a sensitive and accurate analytical method for the determination of trace AFB1 to ensure food safety and human health.

A variety of assay methods have been developed for the determination of AFB1, such as liquid chromatography,[9] lateral flow method,[10] fluorescence immunoassay,[11] surface enhanced Raman spectroscopy,[12] enzyme-linked immunosorbent assay,[13] electrochemical method,[14] and surface plasmon resonance.[15] Among them, the fluorescence method has attracted much attention due to its simplicity, rapidity, and high sensitivity.[16−23] Among them, the ratiometric detection method has received extensive attention because it can effectively eliminate the influence of various irrelevant factors (such as probe concentration, instrument efficiency, environmental interference) and greatly improve the accuracy, as it has valid internal reference and there by the output results only depend on analyte.[24,25] However, most fluorescence methods require continuous excitation by an external light source and are thus difficult to avoid the autofluorescence interference from complex matrixes of food samples.[26,27] Therefore, it is necessary to develop a flexible, simple, selective, and sensitive method for the determination of AFB1 in complicated food samples without autofluorescence and exogenous interference.

Persistent luminescent nanoparticles (PLNP) can store excitation energy and then slowly release the trapped carriers to emit long-lasting phosphorescence without continuous excitation.[28,29] PLNP, therefore, can efficiently avoid the autofluorescence interference of a complicated sample due to

Received: February 22, 2022
Accepted: April 1, 2022
Published: April 13, 2022

https://doi.org/10.1021/acs.analchem.2c00861
Anal. Chem. 2022, 94, 6387−6393

no need for real-time excitation, leading to a high signal-to-noise ratio detection.[30,31] Up until now, various PLNP-based probes have been developed for biosensing,[32] bioimaging,[33] and theranostics.[34] Although a ratiometric sensor based on two different PLNP materials to provide dual signals was reported, a tedious preparation process and complex control of experimental conditions were required in such a ratiometric sensor to ensure the stability of the detection signal.[35] Therefore, there is an urgent need to develop endogenous a dual-emissive PLNP-based ratiometric sensor with simple preparation, easy operation, and more stable optical properties.

Herein, we report a ratiometric luminescence aptasensor based on an endogenous dual-emissive PLNP for autofluorescence- and exogenous interference-free detection of AFB1 in food samples. Dual-emissive PLNP $ZnGa_2O_4:Cr_{0.0001}$ was prepared as the light source to give two emissions at 714 and 508 nm as the detection and reference signals, respectively. The aptamer of AFB1 was grafted on the surface of the PLNP to offer the specificity to AFB1, and Cy5.5-modified aptamer cDNA was then hybridized with aptamer through base complementary pairing to give a turn-on ratiometric luminescence aptasensors for AFB1. The developed ratiometric aptasensor not only has the characteristics of needless in situ excitation, autofluorescence- and exogenous interference-free, but also possesses ultrahigh specificity to realize selective and accurate detection of AFB1 in food samples.

EXPERIMENTAL SECTION

Chemicals and Materials. $Zn(NO_3)_2{\cdot}6H_2O$, $Cr(NO_3)_3$, Ga_2O_3, cetyltrimethylammonium bromide (CTAB), 3-aminopropyltriethoxysilane (APTES), ethanol, *N,N*-dimethylformamide (DMF), 4-(2-hydroxyethyl)-1-piperazineethanesulfonic acid (HEPES), and $NH_3{\cdot}H_2O$ were obtained from Sinopharn Chemical Regents Co. Ltd. (Shanghai, China). Sulfo-*N*-succinimidyl-4-(maleimidomethyl) cyclohexane-1-carboxylate ester sodium salt (Sulfo-SMCC) was acquired from Aladdin (Shanghai, China). Sulfhydryl-functionalized AFB1 aptamer and its part cDNA modified with Cy5.5 (cDNA-Cy5.5) (Table S1) were bought from Shanghai Sangon Biological Science & Technology (Shanghai, China). AFB1, deoxynivalenol (DON), fumonisin (FB), ochratoxin A (OTA), and patulin (PAT) were purchased from Pribolab (Qingdao, China). A certified reference material (SP1108004a) (corn powder) was offered by Meizheng Biotechnology Co. Ltd. Ultrapure water was provided by Wahaha Group Co. Ltd. (Hangzhou, China). Phosphate-buffered saline (PBS) solution (10 mM phosphate, 100 mM NaCl, pH 8.0) and Tris-HCl buffer solution (10 mM Tris, 150 mM NaCl, 10 mM KCl, 2.5 mM $MgCl_2$, pH 7.8) were used as the working buffers.

Instrumentation. All luminescence spectra were acquired on a F-7000 fluorescence spectrophotometer (Hitachi, Japan). Transmission electron microscopic (TEM) images were collected on a JEM-2100 transmission electron microscope (JEOL, Japan). X-ray diffraction spectra were recorded on a D2 PHASER diffractometer (Bruker AXS, Germany). Hydrodynamic size distribution and ζ potential were measured on a Nano-ZSE Zetasizer (Malvern, U.K.). Absorption spectra were performed on a UV-3600 PLUS UV−vis-NIR spectrophotometer (Shimadzu Co., Japan). The afterglow decay curves of an aqueous solution were obtained on an IVIS Lumina III imaging system (PerkinElmer, USA).

Synthesis of Dual-Emissive PLNP. The dual-emissive PLNP $ZnGa_2O_4:Cr_{0.0001}$ was prepared according to our previous work with a hydrothermal approach.[36] A total of 30.72 mg of CTAB was dispersed in ultrapure water. A volume of 24 mL of $Ga(NO_3)_3$ (0.4 M), 1.428 g of $Zn(NO_3)_2{\cdot}6H_2O$, and 48 μL of $Cr(NO_3)_3$ (0.01 M) were added to the above solution in turn with vigorous stirring. The resulting solution was adjusted to pH 8.0 immediately with $NH_3{\cdot}H_2O$ and then transferred to a 50 mL Teflon-lined autoclave. The resulting mixture was kept at 220 °C for 24 h after 30 min ultrasonication and 90 min vigorous stirring. After cooling to room temperature, the product was collected by centrifugation at 9020*g* for 10 min and washed alternately with ethanol and water for 6 times and then lyophilized. Finally, the resulting PLNP was obtained after 1 h calcination in a muffle furnace at 600 °C.

Preparation of Aptamer-Modified PLNP (PLNP-apt). Hydroxyl and amino functionalized PLNP (PLNP-OH and PLNP-NH_2, respectively) were obtained according to our previous reports for subsequent preparation of the aptamer-modified PLNP (Figures S1−S3).[37] A total of 2 mg of PLNP-NH_2 and 0.6 mg of Sulfo-SMCC were dispersed in 2 mL of HEPES buffer (10 mM, pH 7.2). The mixture was then incubated under gentle shaking at room temperature for 2 h. The resulting maleimide-functionalized PLNP was collected by centrifugation, washed with PBS three times, and then redispersed in 2 mL of PBS. A total of 4 nmol of AFB1 aptamer was added into the above dispersion and incubated under room temperature shaking for 12 h to offer PLNP-apt. The produced PLNP-apt was collected by centrifugation and washed with PBS three times and redispersed in 2 mL of PBS for further use.

Fabrication of the Ratiometric Aptasensor. PLNP-apt (0.5 mg mL^{-1}, 1 mL) was incubated with 2 nmol of cDNA-Cy5.5 under shaking at 37 °C for 2 h to give cDNA functionalized PLNP-apt (PLNP@Cy5.5) as the ratiometric luminescence aptasensor. The resulting PLNP@Cy5.5 was separated by centrifugation, washed with PBS thrice, and redispersed in 2 mL of Tris-HCl buffer.

Collection and Preparation of Food Samples. Food samples (corn, wheat, oats, millet, peanuts, and wheat kernels) were purchased from local supermarkets and crushed into powder with a multifunctional crusher. The sample extract was prepared according to the previous publication[38] and the National Food Safety Standards of China (GB5009.22-2016). Briefly, the food sample (5 g) was first dispersed in 20 mL of acetonitrile/H_2O solution (84/16, v/v) with 20 min ultrasonication, followed by 20 min vigorous shaking. The mixture was then centrifuged at 9020*g* for 15 min to remove the residue. The resulting supernatants were filtered with a 0.22 μm filter membrane and made up to 100 mL with Tris-HCl buffer before analysis. In total, 5 g of certified reference corn powder (SP1108004a) was pretreated with the above method.

Determination of AFB1. A volume of 50 μL of AFB1 standard solution (or sample solution) was mixed with 100 μL of PLNP@Cy5.5 (1 mg mL^{-1}) and made up to 500 μL with Tris-HCl buffer. The mixture was incubated at 37 °C under gentle shaking for 40 min. After that, the resulting solution was dispersed evenly, and the luminescence intensity at 508 and 714 nm of the solution was measured for the ratiometric determination of AFB1 on an F-7000 fluorescence spectrometer in the phosphorescence mode.

https://doi.org/10.1021/acs.analchem.2c00861
Anal. Chem. 2022, 94, 6387−6393

RESULTS AND DISCUSSION

Design and Fabrication of the Ratiometric Aptasensor. The ratiometric luminescence aptasensor is designed based on dual-emissive PLNP integrated with AFB1-aptamer (Scheme 1). The dual-emissive PLNP $ZnGa_2O_4:Cr_{0.0001}$ is

Scheme 1. Illustration of the Design and Principle of the PLNP@Cy5.5 Ratiometric Luminescence Aptasensor for the Detection of AFB1

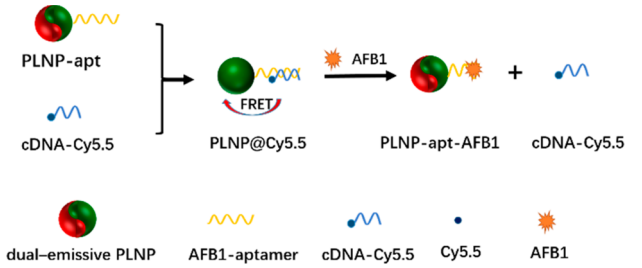

employed as the detection and reference signal unit of the ratiometric aptasensor because of its advantages of no need for in situ excitation and no background interference effect.[35] To achieve high specificity of the ratiometric aptasensor, sulfhydryl terminal AFB1 aptamer was conjugated with PLNP-NH_2 via Sulfo-SMCC as the cross-linking reagent to give PLNP-apt. cDNA-Cy5.5 is finally hybridized with PLNP-apt through base complementary pairing to form a turn on ratiometric luminescence aptasensor (PLNP@Cy5.5). The luminescence at 714 nm is quenched in PLNP@Cy5.5 due to the overlap of the absorption of Cy5.5 and the emission of PLNP at 714 nm (Figure S4). In the presence of AFB1, the AFB1 aptamer preferentially binds with AFB1 to make PLNP@Cy5.5 release cDNA-Cy5.5 to form PLNP-apt-AFB1, resulting in AFB1 concentration-dependent luminescence recovery at 714 nm with AFB1-independent luminescence at 508 nm as the reference signal. As such, the as-designed PLNP@Cy5.5 ratiometric aptasensor integrates the unique luminescence performance of dual-emissive PLNP and the specificity of aptamer.

Characterization of Dual-Emissive PLNP. The as-prepared PLNP had highly crystalline cubic spinel nanoparticles (Figure 1A) with diameters of 25 ± 3 nm (Figure S5) and gave two emission peaks at 508 and 714 nm for the natural defects in the matrix of zinc gallate and the $^2E \rightarrow {}^4A_2$ transition of twisted Cr^{3+}, respectively (Figure 1B, Figure S6).[35] Besides, the dual-emissive PLNP had long-lasting and repeatable afterglow at 508 and 714 nm upon 254 nm UV light excitation for 5 min (Figure 1C). Although the luminescence of each emission peak was greatly affected by the concentration of PLNP and the test conditions such as test voltage, the intensity ratio of the two emissions (I_{714}/I_{508}) was generally stable under different conditions (Figure 1D,E and Figures S7 and S8), effectively eliminating the interference of experimental parameters in a single-emissive probe. In addition, the afterglow intensity of each emission peak decayed rapidly with time, whereas the ratio of the afterglow intensity of the two emission peaks (I_{714}/I_{508}) was still kept constant (Figure 1F), avoiding the influence of the detection time window on the luminescence in single-emissive PLNPs. The above results clearly show that the as-prepared dual-emissive PLNP has a tremendous potential for ratiometric sensing with easy

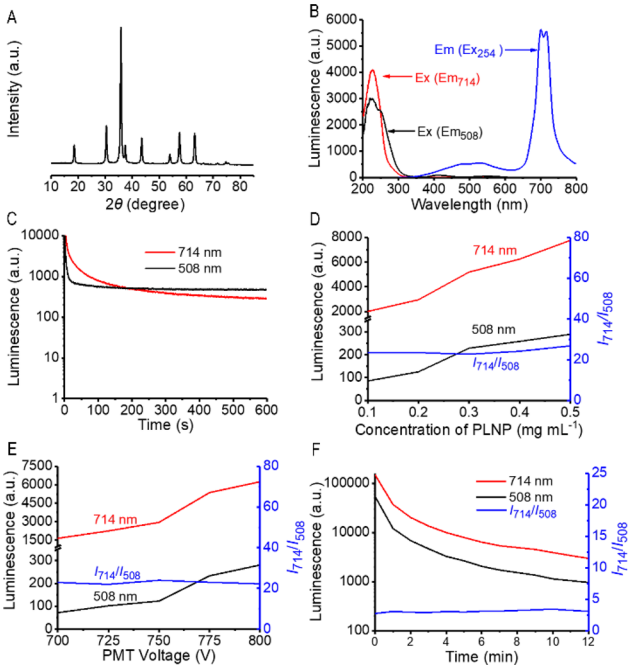

Figure 1. (A) XRD pattern of the as-prepared PLNP. (B) Excitation (emission at 508 and 714 nm) and emission (excitation at 254 nm) spectra. (C) Afterglow decay curves for the emissions at 508 and 714 nm after 5 min 254 nm UV irradiation. (D) Effect of the concentration of PLNP (0.1−0.5 mg mL^{-1}) on the luminescence intensity of 714 and 508 nm and the luminescence ratio I_{714}/I_{508}. (E) Effect of the test voltage on the luminescence intensity of 714 and 508 nm and the luminescence ratio (I_{714}/I_{508}) (0.2 mg mL^{-1}). (F) Afterglow and luminescence ratio (I_{714}/I_{508}) decay curves obtained from an IVIS Lumina III imaging system (0.2 mg mL^{-1}).

operation, with no interference from autofluorescence and experimental factors.

Preparation and Characterization of PLNP-Apt. The effects of reaction time, pH of the reaction system and the concentration of aptamer on the cross-linking reaction of PLNPs and aptamer were studied. The influence of reaction time and pH was investigated first with 1 mg mL^{-1} of PLNP-NH_2 (1 mL) and 2 nmol of AFB1 aptamer in PBS with different pH values (7.4, 8.0, and 8.5). With the increase of reaction time, the absorbance of aptamer at 260 nm in the reaction supernatant gradually decreased and reached a stable level at 12 h (Figure 2A), indicating that 12 h was sufficient for the cross-linking reaction of PLNP-NH_2 and aptamer. Besides, the optimal pH was 8.0 for the cross-linking reaction (Figure 2A). The amount of AFB1-aptamer was subsequently optimized with 1 mg mL^{-1} of PLNP-NH_2 (1 mL) and 12-h reaction in PBS (pH 8.0). As the concentration of AFB1 aptamer increased, the absorbance change of the aptamer at 260 nm before and after reaction gradually increased and leveled off over 2 nmol mL^{-1}, suggesting that 2 nmol mL^{-1} of aptamer was sufficient for the reaction with PLNP-NH_2 to form PLNP-apt (Figure 2B). As a result, the hydrodynamic diameter and the zeta potential of PLNP-NH_2 increased from 106.0 ± 22.7 nm to 142.0 ± 33.7 nm and turned from 17.13 ± 0.29 to −38.20 ± 1.67, respectively, further confirming the successful preparation of PLNP-apt (Figure S9 and Figure 2C). The coupling efficiency of AFB1 aptamer on PLNP was 11.4% (Figure S10).

https://doi.org/10.1021/acs.analchem.2c00861
Anal. Chem. 2022, 94, 6387−6393

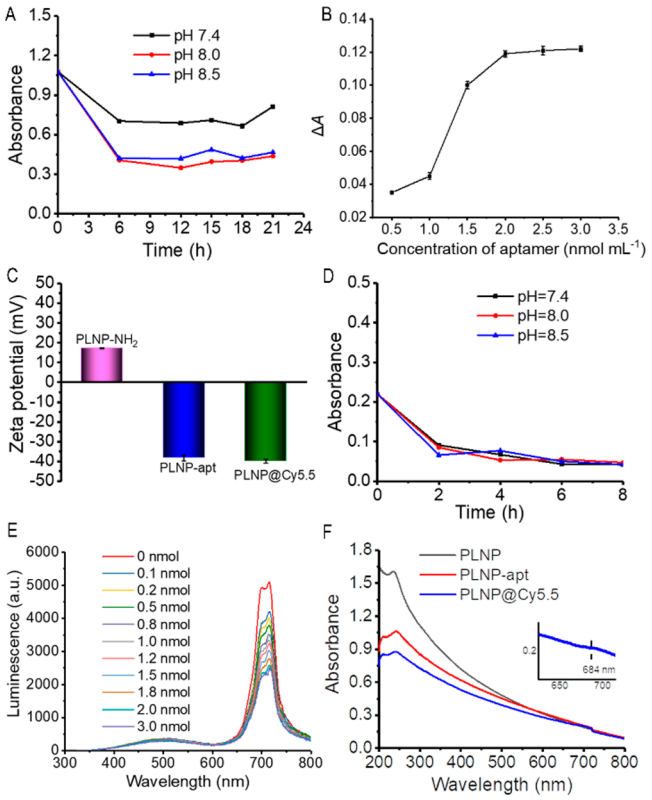

Figure 2. (A) Effect of reaction time and pH on the absorbance of aptamer in the supernatant of PLNP incubated with aptamer at different pHs. (B) Absorbance change of different concentrations of aptamer after conjugation with PLNP (0.5 mg mL^{-1}). (C) Zeta potential of PLNP-NH_2, PLNP-apt, and PLNP@Cy5.5. (D) Time-dependent absorbance of cDNA-Cy5.5 in the supernatant of PLNP-apt incubated with cDNA-Cy5.5 at different pHs. (E) Effect of the amount of cDNA-Cy5.5 on the luminescent intensity of PLNP@Cy5.5 (0.5 mg mL^{-1}) with hybridization. (F) UV−vis-NIR absorption spectra of PLNP, PLNP-apt, and PLNP@Cy5.5.

Fabrication and Characterization of PLNP@Cy5.5. The effects of reaction time, pH of the reaction system, and the concentration of cDNA-Cy5.5 on the hybridization of PLNP-apt and cDNA-Cy5.5 were also optimized. The influence of reaction time on the hybridization was first investigated with 0.5 mg mL^{-1} of PLNP-apt (1 mL) and 2 nmol of cDNA-Cy5.5 in PBS with different pH values (pH 7.4, 8.0, and 8.5). The absorbance of Cy5.5 at 684 nm in the reaction supernatant gradually decreased as the reaction time increased up to 2 h and then leveled off. Meanwhile, the luminescence intensity at 714 nm originating from the PLNP also gradually decreased due to the Förster resonance energy transfer (FRET) from PLNP to Cy5.5 caused by the formation of PLNP@Cy5.5 and reached a minimum at 2 h. However, the pH of the reaction system has little effect on the hybridization (Figure 2D). For convenience, the same PBS solution (pH 8.0) as for the cross-linking reaction and 2 h reaction time were selected for the hybridization. The influence of the amount of cDNA-Cy5.5 on the luminescence intensity of 0.5 mg mL^{-1} PLNP-Apt (1 mL) was then studied. As the amount of cDNA-Cy5.5 increased, the luminescence intensity at 714 nm gradually decreased due to the FRET effect between PLNP and Cy5.5, while the luminescence intensity at 508 nm remained constant (Figure 2E), holding great promise for luminescence ratiometric sensing. Since excessive cDNA-Cy5.5 could affect the sensitivity of the aptasensor to AFB1, 2 nmol of cDNA-Cy5.5 was selected to build PLNP@Cy5.5.

Dynamic light scattering, zeta potential analysis, and ultraviolet−vis-near-infrared (UV−vis-NIR) absorption spectra further confirmed the successful preparation of PLNP@Cy5.5. Compared with PLNP-apt, the developed PLNP@Cy5.5 gave a larger hydrodynamic size (164.0 ± 23.1 nm), but no obvious change in zeta potential (Figure S9, Figure 2C). Besides, PLNP-cDNA showed a characteristic absorption peak at ∼684 nm originating from cDNA-Cy5.5 (Figure 2F).

To make sure whether PLNP@Cy5.5 still has autofluorescence and exogenous interference-free properties, the change in luminescence intensity at each emission (714 and 508 nm) and the luminescence ratio (I_{714}/I_{508}) with the concentration of PLNP@Cy5.5 and test voltage were investigated. Like the naked PLNP, the intensity of the two emission peaks increased with the increase of concentration and voltage, but the luminescence ratio I_{714}/I_{508} remained constant (Figure 3A,B; Figures S11 and S12). Besides, the afterglow decay curve of the prepared PLNP@Cy5.5 was recorded on the Lumina III imaging system subsequently, and the results also showed no significant change of the luminescence ratio I_{714}/I_{508} over time (Figure 3C). Besides, the as-prepared PLNP@Cy5.5 had great stability in Tris-HCl buffer, with no obvious change in luminescence intensity and the hydrodynamic size within 7 days (Figure S13). The above results fully confirm that the prepared PLNP@Cy5.5 has the features of no autofluor-

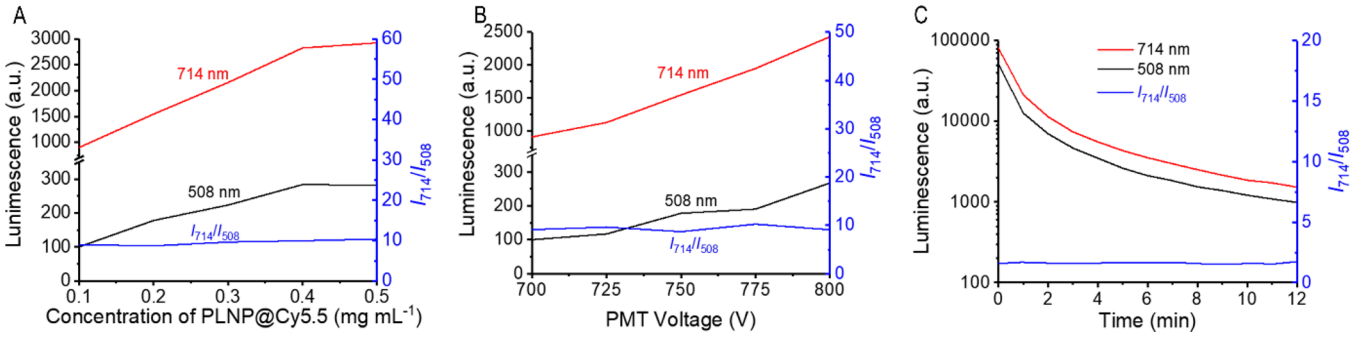

Figure 3. (A) Effect of concentration of PLNP@Cy5.5 (0.1−0.5 mg mL^{-1}) on the luminescence intensity of 714 and 508 nm and the luminescence ratio of I_{714}/I_{508}. (B) Effect of test voltage on the luminescence intensity (714 and 508 nm) and the luminescence ratio (I_{714}/I_{508}) of PLNP@Cy5.5 (0.2 mg mL^{-1}). (C) Effect of test time on the luminescence intensity (714 and 508 nm) and the luminescence ratio (I_{714}/I_{508}) of PLNP@Cy5.5 obtained from an IVIS Lumina III imaging system.

https://doi.org/10.1021/acs.analchem.2c00861
Anal. Chem. 2022, 94, 6387−6393

escence and exogenous interferences, showing a good prospect for ratiometric sensing.

Optimization of AFB1 Sensing. pH is important for the sensitivity of PLNP@Cy5.5 to the target AFB1. Thus, the effect of pH on the luminescence ratio I_{714}/I_{508} of PLNP@Cy5.5 mixed with 20 ng mL^{-1} of AFB1 was investigated first. The change in the luminescence ratio ($\Delta(I_{714}/I_{508})$) due to AFB1 reached the maximum at pH 7.8 (Figure 4A).

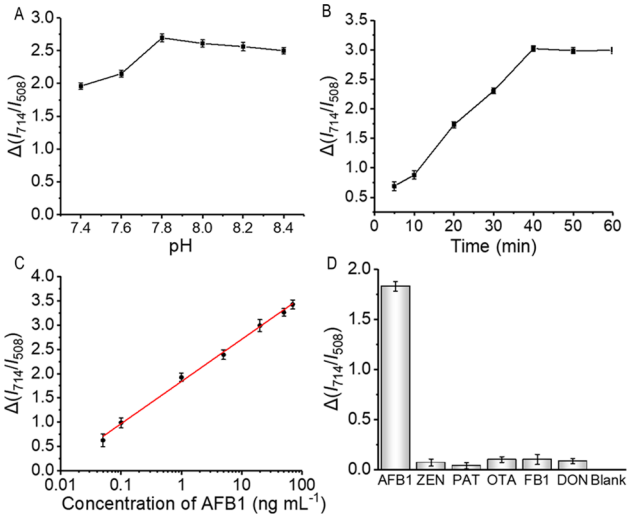

Figure 4. (A) Effect of pH on the $\Delta(I_{714}/I_{508})$ of the aptasensor. (B) Effect of reaction time on the $\Delta(I_{714}/I_{508})$ of the aptasensor. (C) Plot of $\Delta(I_{714}/I_{508})$ against the concentration of AFB1. (D) Selectivity for the detection of AFB1 (AFB1, 1 ng mL^{-1}; all other toxins, 100 ng mL^{-1}).

Additionally, the effect of kinetic curves between PLNP@Cy5.5 and AFB1 was investigated at pH 7.8. $\Delta(I_{714}/I_{508})$ increased rapidly with reaction time, then remained unchanged over 40 min (Figure 4B). Thus, pH 7.8 and 40 min reaction time was taken for AFB1 sensing.

Figures of Merit for the Developed Ratiometric Luminescence Aptasensor. The performance of the developed PLNP@Cy5.5 ratiometric luminescence aptasensor was investigated under the optimal conditions. As the concentration of AFB1 increased, the luminescence intensity at 714 nm gradually increased whereas the luminescence intensity at 508 nm remained stable (Figures S14 and S15). Importantly, in the range of AFB1 concentration from 0.05 ng mL^{-1} to 70 ng mL^{-1}, $\Delta(I_{714}/I_{508})$ had a good linear relationship with the logarithmic concentration of AFB1 (Figure 4C) with a determination coefficient (R^2) of 0.9973. The limit of detection (LOD) (3 s) was 0.016 ng mL^{-1}, and the precision of 1 ng mL^{-1} AFB1 was 2.3% (relative standard deviation for 11 replicate determinations). The results showed that the ratiometric luminescence aptasensor could avoid the autofluorescence interference of matrix and fluctuation of signal caused by external factors due to the no need for in situ excitation and the presence of the reference signal at 508 nm. The developed ratiometric aptasensor gave a wider linear range and much lower LOD than some methods for AFB1 determination (Table S2).

Selectivity of the Developed Ratiometric Luminescence Aptasensor. To investigate the specificity of the developed ratiometric luminescence aptasensor for AFB1, the interference of other mycotoxins including OTA, FB1, ZEN, PAT, and DON was investigated with 100 times higher concentration of AFB1. An obvious change of $\Delta(I_{714}/I_{508})$ was observed only in the presence of AFB1, demonstrating the great specificity of the ratiometric luminescence aptasensor for AFB1 (Figure 4D).

Method Validation and Application to Real Sample Analysis. The accuracy of the proposed ratiometric luminescence aptasensor was verified by analyzing a certified AFB1 reference material (SP1108004a) (corn powder). The concentration of AFB1 (40.1 ± 4.6 μg kg^{-1}, n = 5) determined by the developed ratiometric luminescence aptasensor with a simple aqueous standard calibration was in good agreement with the certified value (41.7 ± 7.5 μg kg^{-1}), proving the accuracy of the proposed aptsensor for interference-free determination of AFB1. The developed luminescence aptsensor was then applied to the ratiometric determination of AFB1 in millet, oats, corn, wheat, wheat kernel, and peanut samples. AFB1 was detected only in the millet sample. The recoveries of spiked AFB1 in the above samples were 95.1–106.5% (Table 1), indicating that the detection of AFB1 was accurate without significant interference.

Table 1. Analytical Results for the Determination of AFB1 in Food Samples[a]

samples	spiked AFB1 (μg kg^{-1})	concentration determined (μg kg^{-1}, mean ± s, n = 5)	recovery (%, mean ± s, n = 5)
millet	0	0.820 ± 0.010	
	3.2	3.931 ± 0.203	97.8 ± 6.3
	6.4	6.973 ± 0.159	96.3 ± 2.5
	12.8	12.95 ± 0.45	95.1 ± 3.5
oats	0	ND	
	3.2	3.311 ± 0.194	103.5 ± 6.1
	6.4	6.221 ± 0.251	97.2 ± 5.7
	12.8	12.65 ± 0.57	98.8 ± 4.4
corn	0	ND	
	3.2	3.152 ± 0.113	98.5 ± 3.5
	6.4	6.451 ± 0.135	100.8 ± 4.1
	12.8	13.35 ± 0.48	104.3 ± 3.8
wheat	0	ND	
	3.2	3.351 ± 0.143	104.7 ± 4.5
	6.4	6.227 ± 0.149	97.3 ± 2.9
	12.8	12.99 ± 0.36	101.5 ± 2.8
wheat kernel	0	ND	
	3.2	3.158 ± 0.221	98.7 ± 6.9
	6.4	6.080 ± 0.212	95.0 ± 3.3
	12.8	13.02 ± 0.42	101.7 ± 3.3
peanut	0	ND	
	3.2	3.407 ± 0.115	106.5 ± 3.6
	6.4	6.470 ± 0.126	101.1 ± 6.5
	12.8	12.33 ± 0.33	96.4 ± 2.6

[a]ND: not detected.

CONCLUSIONS

We have reported a dual-emissive PLNP-based ratiometric luminescence aptasensor for autofluorescence- and exogenous interference-free determination of AFB1 in food samples. The proposed ratiometric luminescence aptasensor integrates the merits of needless in situ excitation, no autofluorescence- and exogenous interference, along with high sensitivity and selectivity, holding great potential for accurate determination

https://doi.org/10.1021/acs.analchem.2c00861
Anal. Chem. 2022, 94, 6387−6393

of trace AFB1 in complex matrixes. In addition, the ratiometric luminescence aptasensor has a good universality for different targets by simply replacing the aptamers and complementary chains, showing a broad application prospect in the field of food analysis and environmental detection.

■ ASSOCIATED CONTENT

Supporting Information

The Supporting Information is available free of charge at https://pubs.acs.org/doi/10.1021/acs.analchem.2c00861.

Additional tables and figures as described in the text; the sequence of aptamer and cDNA; comparison of the developed method with some reported methods for the determination of AFB1; FT-IR spectra, hydrodynamic size, and zeta potential of PLNP, PLNP-OH, and PLNP-NH_2; luminescent spectrum of PLNP and the absorption spectrum of Cy5.5; TEM image; emission spectra of PLNP and PLNP@Cy5.5 with different concentrations and voltages; hydrodynamic size distribution of PLNP-apt and PLNP@Cy5.5; stability of PLNP@Cy5.5; and change of the luminescent signal and luminescence at 508 nm, 714 nm and $\Delta(I_{714}/I_{508})$ with the concentration of AFB1 (PDF)

■ AUTHOR INFORMATION

Corresponding Authors

Xu Zhao − *State Key Laboratory of Food Science and Technology, International Joint Laboratory on Food Safety, Key Laboratory of Synthetic and Biological Colloids, Ministry of Education, School of Chemical and Material Engineering, and Institute of Analytical Food Safety, School of Food Science and Technology, Jiangnan University, Wuxi 214122, China;* orcid.org/0000-0001-8000-9045; Email: zhaoxu2017@jiangnan.edu.cn

Xiu-Ping Yan − *State Key Laboratory of Food Science and Technology, International Joint Laboratory on Food Safety, Key Laboratory of Synthetic and Biological Colloids, Ministry of Education, School of Chemical and Material Engineering, and Institute of Analytical Food Safety, School of Food Science and Technology, Jiangnan University, Wuxi 214122, China;* orcid.org/0000-0001-9953-7681; Email: xpyan@jiangnan.edu.cn

Authors

Lu-Ming Pan − *Key Laboratory of Synthetic and Biological Colloids, Ministry of Education, School of Chemical and Material Engineering and Institute of Analytical Food Safety, School of Food Science and Technology, Jiangnan University, Wuxi 214122, China*

Xiang Wei − *State Key Laboratory of Food Science and Technology, International Joint Laboratory on Food Safety, and Institute of Analytical Food Safety, School of Food Science and Technology, Jiangnan University, Wuxi 214122, China*

Li-Jian Chen − *State Key Laboratory of Food Science and Technology, International Joint Laboratory on Food Safety, and Institute of Analytical Food Safety, School of Food Science and Technology, Jiangnan University, Wuxi 214122, China;* orcid.org/0000-0001-8671-8766

Chan Wang − *Key Laboratory of Synthetic and Biological Colloids, Ministry of Education, School of Chemical and Material Engineering, Jiangnan University, Wuxi 214122, China*

Complete contact information is available at: https://pubs.acs.org/10.1021/acs.analchem.2c00861

Notes

The authors declare no competing financial interest.

■ ACKNOWLEDGMENTS

This work was supported by the National Natural Science Foundation of China (Grant No. 21934002), the National First-class Discipline Program of Food Science and Technology (Grant No. JUFSTR20180301), and the Collaborative Innovation Center of Food Safety and Quality Control in Jiangsu Province.

■ REFERENCES

(1) Gao, J.; Yao, X.; Chen, Y.; Gao, Z.; Zhang, J. *Anal. Chem.* **2021**, *93*, 677−682.
(2) Peng, G.; Li, X.; Cui, F.; Qiu, Q.; Chen, X.; Huang, H. *ACS Appl. Mater. Interfaces* **2018**, *10*, 17551−17559.
(3) Jia, B.; Liao, X.; Sun, C.; Fang, L.; Zhou, L.; Kong, W. *Food Chem.* **2021**, *356*, 129614.
(4) Qian, J.; Ren, C.; Wang, C.; Chen, W.; Lu, X.; Li, H.; Liu, Q.; Hao, N.; Li, H.; Wang, K. *Anal. Chim. Acta* **2018**, *1019*, 119−127.
(5) Guo, X.; Wen, F.; Zheng, N.; Luo, Q.; Wang, H.; Wang, H.; Li, S.; Wang, J. *Biosens. Bioelectron.* **2014**, *56*, 340−344.
(6) Xiong, Z.; Wang, Q.; Xie, Y.; Li, N.; Yun, W.; Yang, L. *Food Chem.* **2021**, *338*, 128122.
(7) Li, Y.; Liu, D.; Meng, S.; Chen, T.; Liu, C.; You, T. *Biosens. Bioelectron.* **2022**, *195*, 113634.
(8) Lu, Y.; Zhang, B.; Tian, Y.; Guo, Q.; Yang, X.; Nie, G. *Microchim. Acta* **2020**, *187*, 467−475.
(9) Somsubsin, S.; Seebunrueng, K.; Boonchiangma, S.; Srijaranai, S. *Talanta* **2018**, *176*, 172−177.
(10) Chen, W.; Cai, F.; Wu, Q.; Wu, Y.; Yao, B.; Xu, J. *Food Chem.* **2020**, *328*, 127081.
(11) Lu, D.; Jiang, H.; Zhang, G.; Luo, Q.; Zhao, Q.; Shi, X. *ACS Appl. Mater. Interfaces.* **2021**, *13*, 25738−25747.
(12) Wu, Z.; Sun, D.-W.; Pu, H.; Wei, Q.; Lin, X. *Food Chem.* **2022**, *372*, 131293.
(13) Wu, L.; Zhou, M.; Wang, Y.; Liu, J. *J. Hazard. Mater.* **2020**, *399*, 123154.
(14) Singh, A. K.; Dhiman, T. K.; Lakshmi, G. B. V. S.; Solanki, P. R. *Bioelectrochemistry* **2021**, *137*, 107684.
(15) Moon, J.; Byun, J.; Kim, H.; Lim, E.-K.; Jeong, J.; Jung, J.; Kang, T. *Sensors* **2018**, *18*, 598.
(16) Yan, X.; Li, H.; Zheng, W.; Su, X. *Anal. Chem.* **2015**, *87*, 8904−8909.
(17) Lu, Z.; Chen, X.; Wang, Y.; Zheng, X.; Li, C.-M. *Microchim. Acta* **2015**, *182*, 571−578.
(18) Wang, C.; Zhang, W.; Qian, J.; Wang, L.; Ren, Y.; Wang, Y.; Xu, M.; Huang, X. *Anal. Methods* **2021**, *13*, 462−468.
(19) Jia, Y.; Wu, F.; Liu, P.; Zhou, G.; Yu, B.; Lou, X.; Xia, F. *Talanta* **2019**, *198*, 71−77.
(20) Wang, C.; Li, Y.; Zhou, C.; Zhao, Q. *Microchim. Acta* **2019**, *186*, 728−732.
(21) Chen, L.; Wen, F.; Li, M.; Guo, X.; Li, S.; Zheng, N.; Wang, J. *Food Chem.* **2017**, *215*, 377−382.
(22) Jia, Y.; Zhou, G.; Wang, X.; Zhang, Y.; Li, Z.; Liu, P.; Yu, B.; Zhang, J. *Talanta* **2020**, *219*, 121342.
(23) Fan, Y.-Y.; Li, J.; Fan, L.; Wen, J.; Zhang, J.; Zhang, Z.-Q. *Sens. Actuators B-Chem.* **2021**, *346*, 130561.
(24) Yu, Y.; Yang, Y.; Ding, J.; Meng, S.; Li, C.; Yin, X. *Anal. Chem.* **2018**, *90*, 13290−13298.
(25) Jin, H.; Gui, R.; Yu, J.; Lv, W.; Wang, Z. *Biosens. Bioelectron.* **2017**, *91*, 523−537.

(26) Wang, B.-B.; Zhao, X.; Chen, L.-J.; Yang, C.; Yan, X.-P. *Anal. Chem.* **2021**, *93*, 2589−2595.
(27) Gui, R.; Jin, H.; Bu, X.; Fu, Y.; Wang, Z.; Liu, Q. *Coord. Chem. Rev.* **2019**, *383*, 82−103.
(28) Song, L.; Li, P.-P.; Yang, W.; Lin, X.-H.; Liang, H.; Chen, X.-F.; Liu, G.; Li, J.; Yang, H.-H. *Adv. Funct. Mater.* **2018**, *28*, 1707496.
(29) Palner, M.; Pu, K.; Shao, S.; Rao, J. *Angew. Chem. Int. Ed.* **2015**, *54*, 11477−11480.
(30) Lv, X.; Chen, N.; Wang, J.; Yuan, Q. *Sci. China. Mater.* **2020**, *63*, 1808−1817.
(31) Wang, J.; Ma, Q.; Zheng, W.; Liu, H.; Yin, C.; Wang, F.; Chen, X.; Yuan, Q.; Tan, W. *ACS Nano* **2017**, *11*, 8185−8191.
(32) Wang, X.; Wang, Y.; Chen, S.; Fu, P.; Lin, Y.; Ye, S.; Long, Y.; Gao, G.; Zheng, J. *Biosens. Bioelectron.* **2022**, *198*, 113849.
(33) Zhang, L.; Lei, J.; Liu, J.; Ma, F.; Ju, H. *Biomaterials* **2015**, *67*, 323−334.
(34) Abdurahman, R.; Yang, C.-X.; Yan, X.-P. *Chem. Commun.* **2016**, *52*, 13303−13306.
(35) Shi, L.; Zheng, W.; Miao, H.; Liu, H.; Jing, X.; Zhao, Y. *Microchim. Acta* **2020**, *187*, 615−625.
(36) Liu, J.-L.; Zhao, X.; Chen, L.-J.; Pan, L.-M.; Yan, X.-P. *Anal. Chem.* **2021**, *93*, 7348−7354.
(37) Abdukayum, A.; Chen, J.-T.; Zhao, Q.; Yan, X.-P. *J. Am. Chem. Soc.* **2013**, *135*, 14125−14133.
(38) Li, J.; Zhao, X.; Chen, L.-J.; Qian, H.-L.; Wang, W.-L.; Yang, C.; Yan, X.-P. *Anal. Chem.* **2019**, *91*, 13191−13197.

https://doi.org/10.1021/acs.analchem.2c00861
Anal. Chem. 2022, 94, 6387−6393